Atmospheric Research 195 (2017) 20–30

Contents lists available at ScienceDirect

Atmospheric Research

journal homepage: www.elsevier.com/locate/atmosres

# Long-term trend in ground-based air temperature and its responses to atmospheric circulation and anthropogenic activity in the Yangtze River Delta, China

Xia Peng[a,c], Qiannan She[b,c], Lingbo Long[b,c], Min Liu[b,c,*], Qian Xu[b], Jiaxin Zhang[b], Weining Xiang[c,d]

[a] School of Geography Sciences, East China Normal University, Shanghai 200241, PR China
[b] School of Ecological and Environmental Sciences, East China Normal University, Shanghai 200241, PR China
[c] Shanghai Key Lab for Urban Ecological Processes and Eco-restoration, East China Normal University, Shanghai 200241, PR China
[d] Center for Ecological Wisdom and Practice Research, College of Architecture and Urban Planning, Tongji University, Shanghai 200092, PR China

ARTICLE INFO

*Keywords:*
Temperature change
Trend analysis
Atmospheric circulation
Anthropogenic activity
Yangtze River Delta

ABSTRACT

The Yangtze River Delta (YRD), including Shanghai City, Jiangsu and Zhejiang Provinces, is the largest metropolitan region in China. In the past decades, the region has experienced massive urbanization and detrimentally affected the environment in the region. Identifying the spatio-temporal variations of climate change and its influencing mechanism in the YRD is an important task for assessing their impacts on the local society and ecosystem. Based on long-term (1958–2014) observation data of meteorological stations, three temperature indices, i.e. extreme maximum temperature (TXx), extreme minimum temperature (TNn), and mean temperature (TMm), were selected and spatialized with climatological calculations and spatial techniques. Evolution and spatial heterogeneity of three temperature indices over YRD as well as their links to atmospheric circulation and anthropogenic activity were investigated. In the whole YRD, a statistically significant overall uptrend could be detected in three temperature indices with the Mann-Kendall (M-K) trend test method. The linear increasing trend for TMm was 0.31 °C/10 a, which was higher than the global average (0.12 °C/10 a during 1951–2012). For TXx and TNn, the increasing rates were 0.41 °C/10 a and 0.52 °C/10 a. Partial correlation analysis indicated that TMm was more related with TXx ($r_p$ = 0.68, $p$ < 0.001) than TNn ($r_p$ = 0.48, $p$ < 0.001). Furthermore, it was detected with M-K analysis at pixel scale that 62.17%, 96.75% and 97.05% of the areas in the YRD showed significant increasing trends for TXx, TNn and TMm, respectively. The increasing trend was more obvious in the southern mountainous areas than the northern plains areas. Further analysis indicated that the variation of TXx over YRD was mainly influenced by anthropogenic activities (e.g. economic development), while TNn was more affected by atmospheric circulations (e.g., the Eurasian zonal circulation index (EAZ) and the cold air activity index (CA)). For TMm, it was a result of comprehensive effects of both atmospheric circulations and anthropogenic activities. On the whole, the northern plain areas was mainly dominated by atmospheric circulations, while the southern mountain areas of YRD was more affected by anthropogenic activities. The findings of this study might help to build a better understanding of the mechanics of temperature variations, and assess the potentially influencing factors on temperature changes.

## 1. Introduction

The global and regional climate has been undergoing significant changes. According to the observed temperature records over the last several decades, the averaged surface air temperature at the global scale increased by 0.85 °C during 1880–2012 (IPCC, 2013). Climate change with the notable temperature variations has great impacts on natural processes (i.e. global climatic and hydrologic processes). It also directly impacts human activities, such as agriculture, energy consumption, and human health (Kadioğlu et al., 2001). The occurrence of extreme temperatures is one of the important aspects of long-term temperature trends. The results from Seneviratne et al. (2012) indicate an overall decrease in clod extremes and increase in warm extremes since 1950s. For instance, the famous summer heatwaves of 2003 and

* Corresponding author at: Shanghai Key Laboratory for Urban Ecological Processes and Eco-Restoration, School of Ecological and Environmental Sciences, East China Normal University, Shanghai 200241, PR China.
*E-mail address:* mliu@re.ecnu.edu.cn (M. Liu).

http://dx.doi.org/10.1016/j.atmosres.2017.05.013
Received 17 January 2017; Accepted 21 May 2017
Available online 22 May 2017
0169-8095/ © 2017 Elsevier B.V. All rights reserved.

2007 had significant influences on ecosystems, economies and societies in Europe (Gönençgil and Deniz, 2016). Especially in 2003, a record-breaking heat wave resulted in an excess of over 70,000 heat-related deaths in Western Europe (Robine et al., 2008). As global warming continues, there is an increasing evidence that the extreme heat events are becoming more frequent, more intense and longer lasting (Gao et al., 2015). The extreme weather and climate events also occurred over China in 2003, 2006, 2007, and 2013 (Chen and Fan, 2007; Peng, 2014). Because of tremendous influences of temperature changes on ecological environment, economic and social development worldwide, particularly the temperature extremes, the changing properties of temperature have aroused heated discussions and became an important global issue among international communities and academic researchers in recent few decades (Arnell, 1999; Jones, 2005; Seneviratne et al., 2012).

A large amount of studies have concentrated on the topic of trends in temperature variations over regional or national scales (Jones, 2005; Ruml et al., 2017) and the global scale (Alexander et al., 2006; Donat et al., 2013a) in the past few years. The study objects shifted from average temperatures (Papakostas et al., 2007) to extreme temperatures (Ballester et al., 2010), mostly based on the temperature indices derived by the Expert Team on Climate Change Detection and Indices (ETCCD) (Karl et al., 1999), World Meteorological Organization Commission for Climatology (CCl), and World Climate Research Programme (WCRP) project on Climate Variability and Predictability (CLIVAR). According to Allen et al. (2015), most people throughout the world have been experiencing the relatively small range of projected temperatures (1.5 to 4 °C) on the daily, weekly, and seasonally scale, and many areas of the world experience far greater shorter term variability. However, the changing properties of temperature extremes are different from place to place, and large regional differences in the temperature trend patterns are existed on different scales (Bonsal et al., 2001). For example, the global conclusions performed by Alexander et al. (2006) are not the representative of Europe according to Moberg et al. (2006). Reversely, Moberg et al. (2006) and Jones (2005) both find a warming in the daily minimum temperature and the daily maximum temperature. Temperature variations are influenced by many complex factors (Jansen et al., 2007). There are substantial temperature variations caused by atmospheric circulations and sea surface temperature, such as the Arctic Oscillation (AO), the Western Pacific subtropical high (WPSH) and El Nino Southern Oscillation (ENSO) (Yu and Xie, 2013; Iqbal et al., 2016; Sun et al., 2016). In addition, the regional variations of temperature trends are also driven by land use/land cover (LUCC) changes (Yang et al., 2009), population growth (Balling et al., 2016), and urbanization (Stone et al., 2010). Although there are many studies available addressing the temperature variations, the conclusions about regional temperature variability in different study areas have not only common consensus, but also differences due to their diverse climatic systems and human activities.

The Yangtze River Delta (YRD), one of the largest metropolitan region in China has experienced an unprecedented process of rapid and massive urbanization, which dramatically altered the landscape with high population density (Xie et al., 2010). Some studies have been conducted in or near the YRD on the changes of temperature. For example, Zhang et al. (2010) tried to build the model of the impact of urbanization on the local and regional climate in the YRD. Du et al. (2007) and Xie et al. (2010) analyzed the influence of urbanization on regional climatic trend of temperature in the YRD based on non-radiance-calibrated DMSP/OLS nighttime light imagery. Wang et al. (2014) studied the temporal and spatial variation of the 16 extreme temperature indices in the Yangtze River Basin during the nearly 50 years. Sang (2012) investigated the variability of daily temperature and the urbanization impacts in the YRD during 1958–2007. Shi et al. (2009) and Jiang and Sun (2012) took into consideration urbanization, air-sea interaction and atmospheric circulations in cause analysis. However, most of the present studies on the temperature variations in the YRD were based on the data observed over several meteorological stations. Limited by the number and location of meteorological stations, it is difficult to accurately analyze the spatial variability of temperature. Moreover, most researches mainly considered the influence of anthropogenic signals on temperature variations, while there was a lack of study taking account of the comprehensive effects of atmospheric circulations and human activities.

In this investigation, this paper aims to investigate the spatio-temporal variation characteristics of temperature at the regional scale and reveal their responses to natural atmospheric circulation and human activities in the YRD region. Based on the long-term ground observations of meteorological stations, we calculated and produced three regional temperature indices (i.e. extreme maximum, minimum and mean temperature) from 1958 to 2014, using climatological calculation methods and specialization techniques. The temporal dynamic trends and spatial evolution patterns of three temperature indices at the pixel scale throughout the YRD in recent 60 years were analyzed with Mann-Kendall trend analysis. Moreover, the potential roles of atmospheric circulations and local anthropogenic activities on the long-term trends of temperature variations were also evaluated.

## 2. Study area

The Yangtze River Delta (YRD) (116°29′-123°45′E, 27°14′-35°33′N) is situated in eastern coastal areas of China and includes Jiangsu province, Zhejiang province, and Shanghai municipality, with 25 cities in total (Fig. 1).It covers an area of 210,700 $km^2$, which represents 2.1% of the national land area (China Statistical Yearbook, 2015). The YRD is significantly influenced by the humid subtropical monsoon climate, with four distinct seasons, plenty of sunshine and good rainfall. The northern areas of the YRD are plain, while the rest of the territory has a complex topography comprised of hills, as well as low and medium-high mountains. In addition, the YRD is one of the most developed economic belts in China and still keeps a fast-growth speed presently. The region's population has increased from 75.73 million in 1958 to 103.86 million in 2014, with urbanization ratio (the proportion of urban population to total population) increased from 23.35% to 75.95% during the same period. In 2014, its gross domestic product (GDP) reached CNY 12.88 trillion (USD 1866.6 billion), creating 20.2% the country's gross domestic product (GDP) (China Statistical Yearbook, 2015). Its complex natural environment and rapid urbanization dramatically altered the landscape and detrimentally affected the climate characteristics in the region (Shi et al., 2009; Xie et al., 2010).

## 3. Data and methods

### 3.1. Meteorological data and spatialization method

Meteorological and elevation data were used in this study to calculate and spatialize temperature variables in the YRD. Meteorological data was supplied by the National Climate Center of the China Meteorological Administration (CMA) with 56 meteorological stations over the YRD (Fig. 1, detailed information was provided in Appendix 1). Before publishing the meteorological data, CMA has strictly controlled the data quality, including checking for the mis-written codes and doubtful records, and homogeneity-adjusted. There are few missing values for CMA stations during their observation years. Climate change is manifested not only by changes in average conditions, but also by changes in the occurrence of climate extremes (IPCC, 2013). Therefore, three temperature indices (Table 1), i.e. extreme maximum temperature (TXx), extreme minimum temperature (TNn), and mean temperature (TMm), referred to climate indices of ETCCDI (Karl et al., 1999) and the research of Zhang et al. (2011), were used to describe the temperature variations in the YRD during 1958–2014. Digital Elevation Model (DEM) data with a spatial resolution of 1 km × 1 km, provided by Institute of the Geographic Sciences and

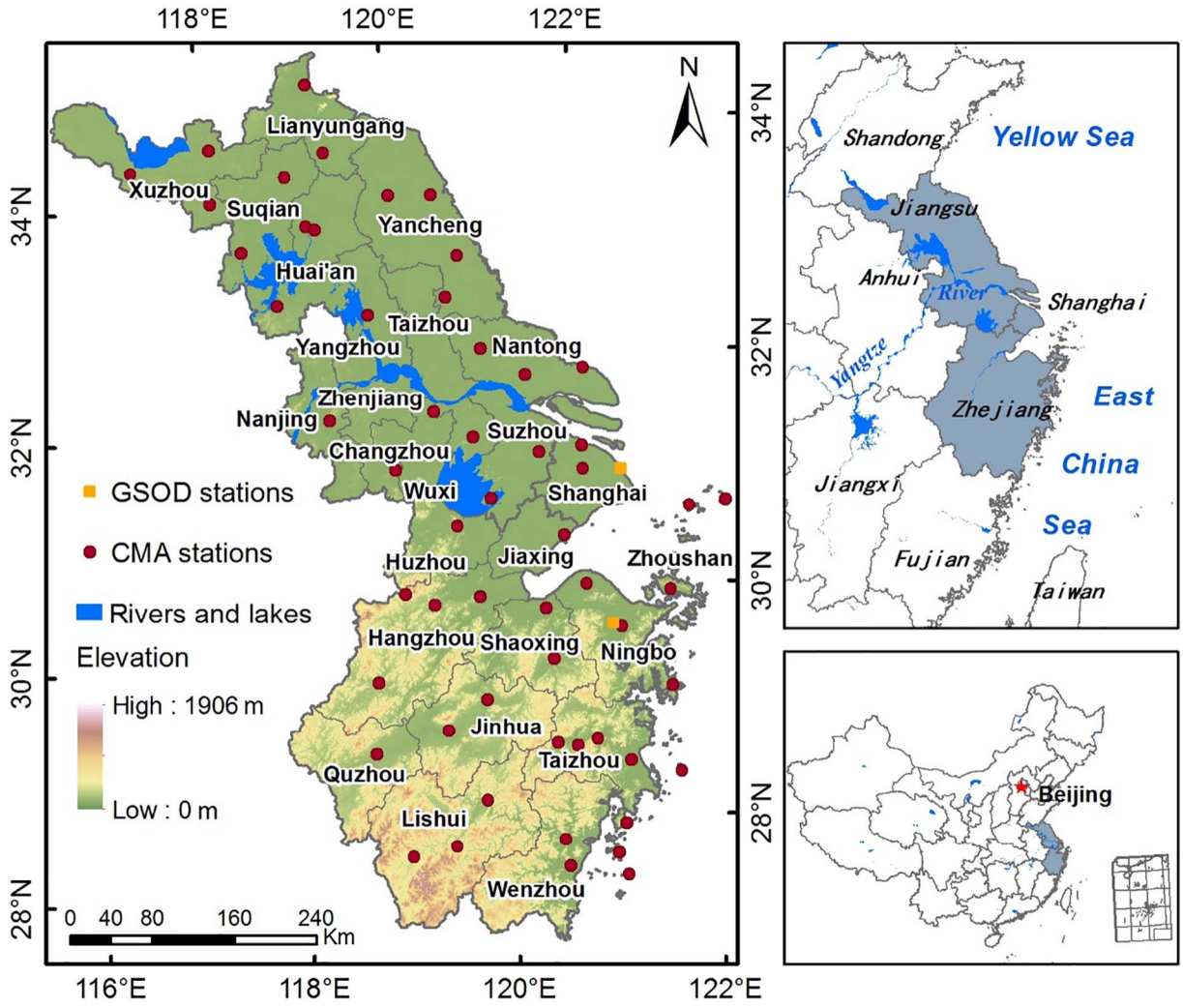


**Fig. 1.** The study area and the locations of meteorological stations over Yangtze River Delta, China. Fifty six stations from the China Meteorological Administration (CMA) and 2 validation stations from the Global Surface Summary of Day datasets (GSOD).

**Table 1**
Definitions of 3 temperature indices used in this study.

| Index | Name | Definition | Units |
|---|---|---|---|
| TXx | Extreme maximum temperature | The maximum of daily maximum temperature | °C |
| TNn | Extreme minimum temperature | The minimum of daily minimum temperature | °C |
| TMm | Mean temperature | The average of daily mean temperature | °C |

Natural Resources Research, was selected as the topographic data for the spatial interpolation of temperature indices.

Australian National University Spline (ANUSPLIN) arithmetic was selected for spatial interpolation of 3 temperature indices over YRD (1 km × 1 km). It was developed by Australian National University (Hutchinson, 1999) and has been widely used in spatial interpolation of meteorological data at various regions and scales (Ogden et al., 2014). The ANUSPLIN package provides a facility for transparent analysis and interpolation of noisy multi-variate data using thin plate smoothing splines, through comprehensive statistical analyses, data diagnostics and spatially distributed standard errors. One of its greatest advantages is that it allows for including terrain factors influencing the climate variable as additional covariates during the interpolation (Sun et al., 2015). The resolution of the final grid is determined by the resolution of the grids of terrain factors (i.e. elevation data in this paper). The influencing factors we took into account in the spatial interpolation of temperature indices included latitude, longitude and elevation.

The Global Surface Summary of Day (GSOD) dataset, provided by the National Climatic Data Center (NCDC) at the National Oceanic and Atmospheric Administration (NOAA) (ftp://ftp.ncdc.noaa.gov/pub/data/gsod/), was used to validate the performance of ANUSPLINE in this study (Kilibarda et al., 2014). As there is a lot of overlap between the two kinds of meteorological datasets (CMA and GSOD), 2 stations different to the CMA dataset, 'Lishe' (121.47°E, 29.83°N) and 'Pudong' (121.81°E, 31.14°N) (the locations as showed in Fig. 1), were selected as the validation sites. And Fig. 2 showed a good agreement between the GSOD observations and the result values with the ANUSPLIN interpolation based on CMA dataset, and the correlation coefficient between them reached 0.89 ($p < 0.05$, N = 36).

### 3.2. Trend analysis with Mann-Kendall method

The time series of three spatialized temperature indices were analyzed at the pixel and regional scales by using Mann-Kendall (M-K) trend analysis method (Mann, 1945; Kendall, 1962). M-K trend analysis is one of the non-parametric statistical test methods (also called distribution-free test methods), having remarkable advantages compared to traditional parametric statistical test methods (Gocic and Trajkovic, 2013). Moreover, this test is less influenced by the presence

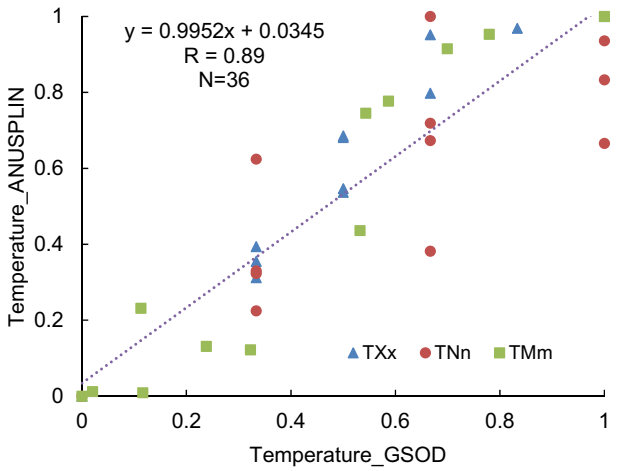


**Fig. 2.** Comparison between 3 temperature indices observed from the GSOD dataset and the spatial interpolation values with ANUSPLIN. TXx: extreme maximum temperature, TNn: extreme minimum temperature, and TMm: mean temperature. All three temperature indices were normalized.

of outliers in the data and relatively easy to calculate (Zhu et al., 2010). Therefore, Mann-Kendall trend analysis has been widely used in time-varying analysis, and recommended by WMO (World Meteorological Organization) in time-varying analysis of environmental data (Yu et al., 2002). The details of M-K test method are presented as follows and the test statistic $S$ is computed by:

$$S = \sum_{i}^{n-1} \sum_{j=i+1}^{n} sgn(x_j - x_i), \tag{1}$$

where $n$ is the length of time series, $x_i$ and $x_j$ are three temperature indices values in time series $i$ and $j (j > i)$, respectively. And $sgn$ is the sign function as:

$$sgn(x_j - x_i) = \begin{cases} 1, & x_j - x_i > 0 \\ 0, & x_j - x_i = 0 \\ -1, & x_j - x_i < 0 \end{cases}, \tag{2}$$

For $n > 10$, $S$ follows a normal distribution with zero mean and variance given by:

$$Var(S) = \frac{n(n-1)(2n+5) - \sum_{k=1}^{n} t_k (t_k - 1)(2t_k + 5)}{18}, \tag{3}$$

where $t_k$ denotes the number of ties of extend $k$. The summation term in the numerator is used only if the data series contains tied values. The standard test statistic $Z_S$ is calculated as follows:

$$Z_S = \begin{cases} \frac{S-1}{\sqrt{Var(S)}}, & (S > 0) \\ 0, & (S = 0), \\ \frac{S+1}{\sqrt{Var(S)}}, & (S < 0) \end{cases} \tag{4}$$

Positive values of $Z_S$ indicate increasing trends while negative $Z_S$ values show decreasing trends. Testing trends are done at the specific α significance level. In this study, significance levels $\alpha = 0.05$ were used. At the 5% significance level, the null hypothesis of no trend is rejected if $Z_S > 1.96$. The magnitude of trend is predicted by the Sen's estimator (Sen, 1968). Here, the slope $\beta$ is computed as:

$$\beta = Median\left[\frac{x_j - x_i}{j - i}\right], \quad \forall\, i < j. \tag{5}$$

### 3.3. Atmospheric circulations and anthropogenic activities

Climate change is not only caused by natural factors but also human activities (Zhang et al., 2011; Balling et al., 2016). A set of 5 atmospheric circulations indexes and 2 anthropogenic activity indicators were selected to evaluate the influences of natural conditions and human activities on the variability of air temperature over the YRD (Table 2). With considering the interdependency of atmospheric circulation indices, 5 of 74 Circulation Index were selected and derived during the study period, which were provided by the Climate Diagnostics and Prediction Division of the National Climate Center (http://cmdp.ncc-cma.net/cn/index.htm) (Shi et al., 2009; Jiang and Sun, 2012), including the Asia polar vortex area index (APVA), the Western Pacific subtropical high area index (WPHA), the Eurasian zonal circulation index (EAZ), the Eurasian meridional circulation index (EAM), and the cold air activity index (CA). The Western Pacific subtropical high pattern is a subtropical anticyclone located in the northwestern portion of the Pacific Ocean, which has significant influences on the East Asian summer climate. The Asia polar vortex pattern is an upper level low-pressure area lying near the Polar Regions and between middle troposphere and stratosphere, which can result in a rapid and dramatic change of weather known as a cold snap. The Eurasian zonal circulation and meridional circulation can enhance the influence of WPHA and APVA, respectively. And the Gross Domestic Product (GDP) and the Gross Population (GP) were used to reflect anthropogenic activities over the YRD from the view of economic and population growth, supplied by National Bureau of Statistics of China (1959–2015).

Based on the statistical theory, if a correlation of two variables is influenced by other variables, the correlation coefficient of the two variables may be misleading. In this study, the partial correlation coefficient ($r_p$) was used to assess the effects of atmospheric circulations and human activity indicators on the temperature variations in the YRD. It measured the degree of association between two variables (e.g.

**Table 2**
Definitions of 5 atmospheric circulation indexes and 2 anthropogenic activity indicators used in this study.

| Type | Influencing factors | Description |
|---|---|---|
| Atmospheric circulations | The Asia polar vortex area index (APVA) | The area of the polar vortex in Asian, which is located in the Northern Hemisphere 500 hPa geopotential height field and is a fan-shaped area enclosed by its southern boundary contour between 60°E-150°E. |
| | The Western Pacific subtropical high area index (WPHA) | The area of the Western Pacific subtropical high, which is located in the Northern Hemisphere 500 hPa geopotential height field and is a spherical area surrounded by ≥ 5880 geopotential meter (gpm) contour between 10°N-60°N, 110°E-180°. |
| | The Eurasian zonal circulation index (EAZ) | The average zonal index in the Northern Hemisphere 500 hPa geopotential height field between 45°N-65°N, 0° -150°E, with an interval of 30° longitudes. |
| | The Eurasian meridional circulation index (EAM) | The average meridional index in the Northern Hemisphere 500 hPa geopotential height field between 45°N-65°N, 0°-150°E, with an interval of 30° longitudes. |
| | The cold air activity index (CA) | The frequency of cold wave processes, i.e. the average temperature drops > 5 °C within 3 consecutive day. |
| Anthropogenic activities | The gross population (GP) | The total population per year. |
| | The gross domestic product (GDP) | The aggregate measure of production equal to the sum of the gross values added of all resident and institutional units engaged in production per year. |

TNn and APVA) without the influence of the other 4 atmospheric circulation indexes and 2 human activity indicators. Therefore, we calculated partial correlation coefficients ($r_p$) of 5 atmospheric circulation indexes, 2 anthropogenic factors and 3 temperature indices. When analyzing the relationship between one of 7 influencing factors (5 atmospheric circulation indexes and 2 anthropogenic activity indicators) and one of 3 temperature indices, the rest of other 6 influencing factors will be set as the control variables. In the case of three variables, the partial correlation coefficient is calculated by:

$$r_{p.ijk} = \frac{r_{ij} - r_{ik} r_{jk}}{\sqrt{(1 - r_{ik}^2)(1 - r_{jk}^2)}}, \quad (6)$$

where $r_{ij}$, $r_{ik}$ and $r_{jk}$ are correlation coefficients between two variables, and $r_{p\_ijk}$ is the partial correlation coefficient between variable $i$ and $j$ with the effect of variable $k$ removed (Zhou et al., 2000). In order to avoid the dimension problem caused by different types of data, all indices, include 3 temperature indices and 7 influencing factors, were converted to $z$-scores (with zero mean and one variance) before the partial correlation analysis. The $z$-scores are computed by:

$$z = \frac{x_i - \mu}{\sigma}, \quad (7)$$

where $z$ is standardized variate, also called the $z$-score, following a normal distribution with zero mean and one variance. And $x_i$ represents the indices of $i$ year, $\mu$ and $\sigma$ indicate the mean and variance of $x$.

## 4. Results and discussion

### 4.1. Spatio-temporal variations of the spatialized temperature indices

The average annual TXx, TNn and TMm for the whole YRD during 1958–2014 were 35.78 °C, −7.77 °C and 15.10 °C, respectively. There was a large spatial heterogeneity of the three temperature indices as shown in Fig. 3a. Overall, extreme maximum temperature (TXx) in YRD was higher in the southern part than that in the northern part. This spatial pattern showed the close correspondence with the topography of YRD. There existed a colder area of TXx lower than 30 °C in the southern mountain areas. Besides, also affected by the topography, the highest TXx of the Jinhua-Quzhou basin, which is located at the junction of Jinhua and Quzhou, reached 38.50 °C. However, for TNn (Fig. 3b) and TMm (Fig. 3c), the spatial pattern characteristics showed temperature was lower in the north and south, while higher in the middle areas. In the north-central plain areas, there was a significant latitudinal variation, more influenced by the geographical location (i.e. latitudes) than the topography. But in the southern mountain areas, the topography played a more important role in the distribution of the annual TNn and TMm. The warm areas mainly concentrated in the central and eastern coastal regions, and the cold regions were distributed in the north and southern mountain areas.

The interannual variations of 3 temperature indices at the entire YRD regional scale were illustrated in Fig. 3d. There existed obvious temperature fluctuations and an overall increasing trend from 1958 to 2014. During the study period, TXx increased by 0.41 °C/10 a ($p < 0.01$) and presented negative anomalies with an obvious periodic variability mostly prior to 2002, then it had a rapid increase after 2003. Moreover, the top two highest TXx appeared in 2013 (40.28 °C, 3.86 °C higher than the average) and 2003 (39.89 °C, 3.47 °C higher than the average), respectively. For TNn, it exhibited a sharp uptrend with a rate of 0.52 °C/10 a ($p < 0.01$). The lowest TNn was appeared in 1969 (−12.52 °C, 4.64 °C lower than the average) and the highest TNn was occurred in 2007 (−4.71 °C, 3.17 °C higher than the average). It should be noted that TNn underwent an obvious decrease in the early 1960s, and a rise with a significant fluctuation in the following decades. Moreover, there existed a turning point occurred in 1990, that TNn was mostly below the average before, while above the average afterwards. And this phenomenon could be also found in TMm. Over the past 57 years, TMm has increased by about 0.31 °C/10 a ($p < 0.01$) in the YRD, and the variations were more moderate before 1990s. However, TMm showed an obvious increasing trend in recent 20 years, which reached the highest value in 2007 (17.12 °C, 1.73 °C higher than the average) and the lowest value in 1976 (14.37 °C, 1.02 °C lower than the average). Additionally, we calculated their partial correlation coefficients ($r_p$) to evaluate the effects of TXx and TNn on TMm variation, respectively. TMm showed a more significant correlation with TXx ($r_p = 0.68$, $p < 0.001$) than TNn ($r_p = 0.48$, $p < 0.001$). Therefore, the increasing TMm was more caused by the increasing TXx than TNn for the regional scale in the YRD. Overall, 3 temperature indices all showed significant increasing trends during 1958–2014. We also noted that the YRD had warmed at a faster rate than the global average (0.12 °C/10 a during 1951–2012 for the globally averaged surface temperature) (IPCC, 2014). In particular, the air temperature experienced a sharp rise after 1990's.

### 4.2. Trend distributions of temperature indices at pixel scale

The trend magnitudes of 3 temperature indices in the YRD were derived from the slope of M-K analysis (Fig. 4). During 1958–2014, most areas (about 62.17%) of the YRD increased in TXx and were mainly located in the south mountain areas (> 0.8 °C/10 a) and the north-central plain regions (< 0.4 °C/10 a), with the largest positive trends (> 1 °C/10 a) in Lishui, Wenzhou and Taizhou (Fig. 4a). Compared with TXx, the extent with an upward trend expanded for TNn (Fig. 4b), accounting for 96.75% of the total. The larger trend magnitudes were concentrated in the northwestern of Jiangsu province and also in the southern mountain areas of Zhejiang province, ranging from 0.4 to 0.8 °C/10 a. However, the remaining areas presented the lower trend magnitudes ranging from 0.2 to 0.4 °C/10 a, which were mainly located in the Hangzhou Bay. For TMm (Fig. 4c), it might show relatively small variation difference, although almost all areas (about 97.05%) in the YRD showed significant trends. Nevertheless, the larger trend magnitudes were also detected in the southern mountain areas of Zhejiang province. Moreover, TMm had a total negative magnitude of about −0.2 °C/10 a in the southwestern of Zhejiang province. Overall, trend analyses of TXx, TNn and TMm in the YRD during the period 1958–2014 revealed widespread significant temperature changes (62.17%, 96.75% and 97.05%, respectively). Furthermore, the larger-magnitude increase of TXx could be found in the southern YRD, and the larger-magnitude increase of TNn was observed mainly in the northwestern of Jiangsu Province and also in the southern YRD. For TMm, there was little difference in the distribution of increasing trend magnitudes. Similar to what other studies have found in the same or many other regions, the YRD has been warming for the recent 60 years responded to the context of global warming (Sang, 2012).

On the whole, TXx, TNn and TMm have increased significantly during 1958–2014 in the YRD. With respect to TXx, the extent with positive significant trends shrunk compared to the other two indices, especially in the north of Jiangsu province. These similar results were generally consistent with what Zhang et al. (2011) found for the same region in China. Besides, many studies indicated that minimum temperature increased more significantly than maximum temperature (Alexander et al., 2006; Allen et al., 2015). Moreover, a noteworthy phenomenon was that the rate of temperature rise in the southern mountain areas was faster than in other lower-elevation areas. In fact, other studies also have come to this conclusion. For example, Pepin et al. (2015) found the evidence that mountain peak regions of the world were warming faster than the surrounding plateaus and lowlands and analyzed the important mechanisms that contribute towards the EDW (elevation-dependent warming) from snow albedo, water vapor changes and radiative flux changes and so on. Taken together, the results would seem to show that not only temperature in different geographical situations, like elevation, latitude, undergone changes of different degree, but also temperature itself, i.e. minimum temperature,

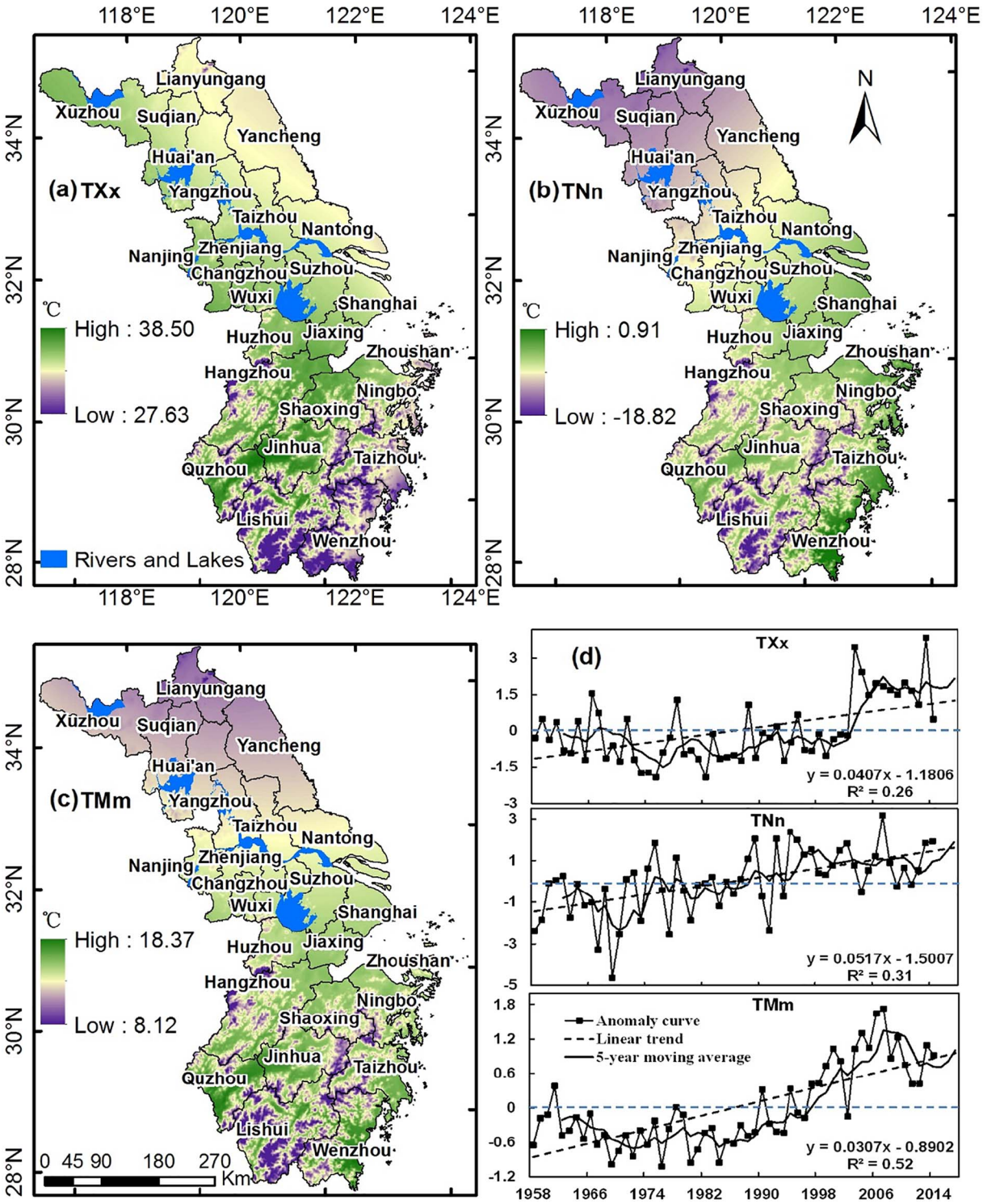


**Fig. 3.** The spatial distributions of TXx (a), TNn (b) and TMm (c) and their variation curves (d) in the YRD from 1958 to 2014. TXx: extreme maximum temperature, TNn: extreme minimum temperature, and TMm: mean temperature.

maximum temperature and mean temperature, presented different sensitivities to the changing environment. As mentioned at Section 4.1, there were different variation characteristics and increasing rates in 3 representative temperature indices.

### 4.3. *Effects of atmospheric circulation and anthropogenic activity on the temperature over YRD*

The partial correlation coefficients ($r_p$) between 3 temperature indices and 7 influencing factors over the YRD were calculated to assess the effects of influencing factors on temperature variations. As shown in Table 3, the increase of GDP in the YRD region had significant positive influences ($r_p$ = 0.45) on the variation of interannual extreme maximum temperature (TXx). As for TNn and TMm, their variations were influenced by both anthropogenic activities (GDP) and atmospheric circulations (APVA, EAZ and CA). EAZ and CA were found to be the atmospheric circulation factors that strongly influenced extreme minimum temperature (TNn) in the whole YRD during 1958–2014.

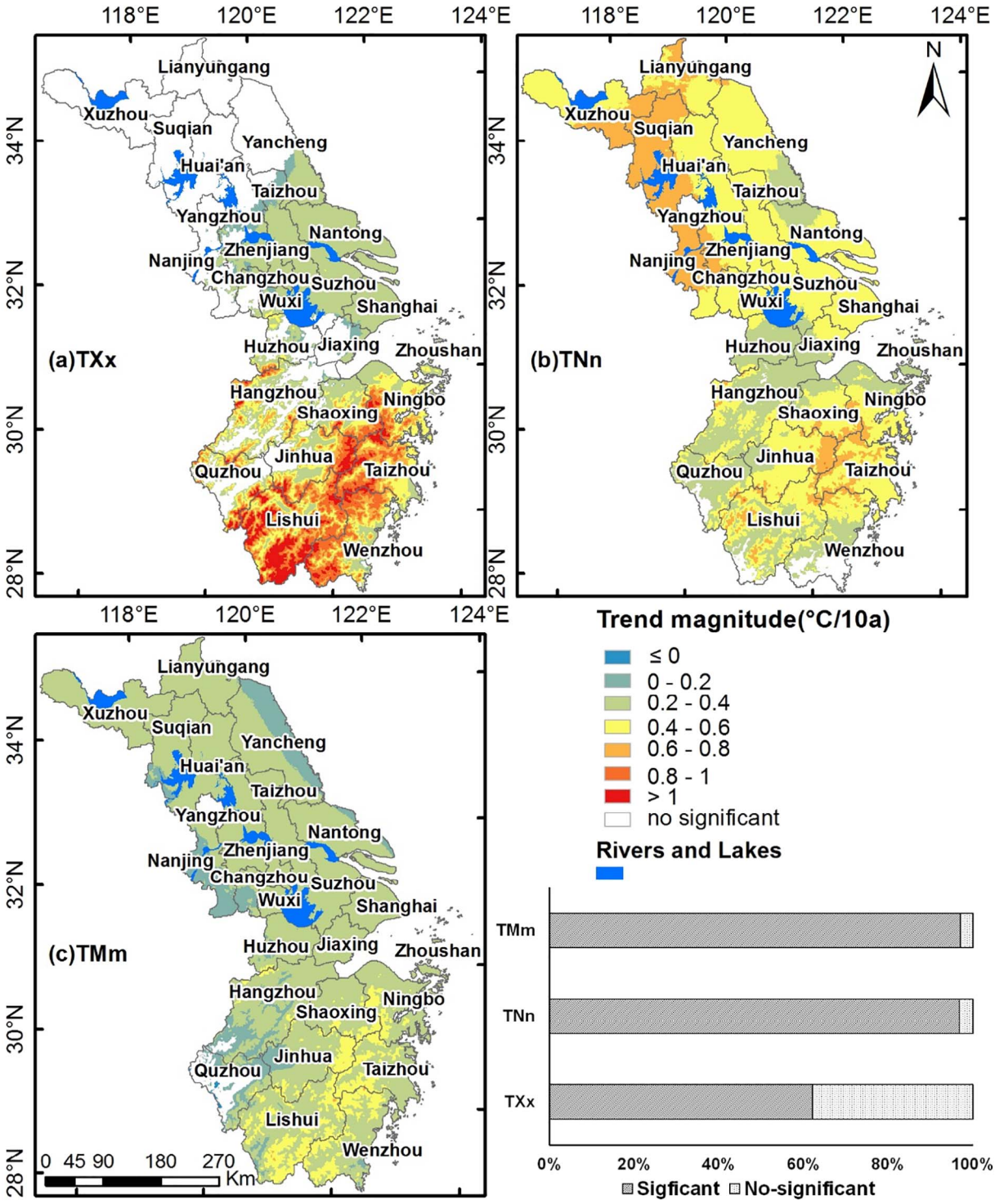


**Fig. 4.** Trends of 3 temperature indices over YRD for the period 1958–2014. (a) TXx: extreme maximum temperature, (b) TNn: extreme minimum temperature, and (c) TMm: mean temperature. Values for trends were significant at the 0.05 level and no-significant were the white areas.

However, APVA and EAZ were the main atmospheric factors which influenced the regional average mean temperature (TMm). It should be noted that GDP also has positive effects on the variations of TNn and TMm. This showed that the development of the local economy did exert considerable influences on increasing of temperature in the YRD. Moreover, for the magnitudes of partial correlation coefficients, it was the evident that human activities played a more important role in the temperature increasing than natural factors. It was similar to Balling et al. (2016), which indicated that the change in population significantly influenced maximum temperatures ($p < 0.05$), not minimum temperatures for Iran during 1961–2010.

The relationships between temperature indices and influencing factors showed the large spatial heterogeneities (Fig. 5). For TXx, WPHA (Fig. 5a), EAM (Fig. 5b), and GDP (Fig. 5c) had significant influences on the interannual TXx variation. Among them, the most widely distributed and strongest factor could be GDP (accounting for 42.53% of the total, and $r_p$ ranged from $-0.35$ to 0.73), as one of the most important anthropogenic influencing factors reflecting the development of urbanization and the increase of energy consumption/gas emission. And the higher $r_p$ between GDP and TXx were concentrated in

**Table 3**
The partial correlation coefficients ($r_p$) between 3 temperature indices and 7 influencing factors in the whole YRD during 1958–2014. TXx: extreme maximum temperature, TNn: extreme minimum temperature, and TMm: mean temperature.

| Type | Influencing factors | TXx | TNn | TMm |
|---|---|---|---|---|
| Atmospheric circulations | The Asia polar vortex area index (APVA) | − 0.06 | 0.05 | − 0.33* |
| | The Western Pacific subtropical high area index (WPHA) | 0.23 | 0.05 | 0.14 |
| | The Eurasian zonal circulation index (EAZ) | − 0.02 | 0.30* | 0.28* |
| | The Eurasian meridional circulation index (EAM) | − 0.22 | − 0.08 | − 0.12 |
| | The cold air activity index (CA) | − 0.01 | − 0.38** | − 0.13 |
| Anthropogenic activities | The gross population (GP) | 0.09 | − 0.09 | 0.19 |
| | The gross domestic product (GDP) | 0.45** | 0.32* | 0.50** |

* $p < 0.05$.
** $p < 0.01$.

the southeastern Zhejiang province, which reached 0.73. For atmospheric circulations, WPHA and EAM positively influenced TXx in the central YRD (i.e. the mouth of the Yangtze River) (accounting for 23.58% of the total, and $r_p$ ranged from 0.28 to 0.45) and negatively correlated with TXx in the northwestern Zhejiang province (accounting for 19.63% of the total, and $r_p$ ranged from − 0.28 to − 0.43), respectively.

As to TNn, we found that the two atmospheric circulation indexes, EAZ (Fig. 5d) and CA (Fig. 5e), were the main atmospheric circulations influencing the variation of extreme minimum temperature (i.e. TNn). TNn was positively correlated with EAZ in the central YRD and the northwestern Zhejiang province (about 43.21%, and $r_p$ ranged from 0.28 to 0.47), particularly in Hangzhou (the highest value, 0.47). CA presented a broad and strong negative influence on TNn in most regions of YRD (about 85.94%, and $r_p$ ranged from − 0.28 to − 0.54), and most significantly in the southern mountain areas of Zhejiang province (with the highest value, − 0.54). For the two anthropogenic factors, TNn was more correlated with GDP (Fig. 5f, about 41.21%, $r_p$ ranged from 0.28 to 0.53) than GP (about 5.72%, $r_p$ ranged from − 0.28 to − 0.37), and higher positive $r_p$ between TNn and GDP existed in the southern YRD. Nevertheless, only a small part of the western Zhejiang province (i.e. in Hangzhou) showed negative $r_p$ between TNn and GP. Thus, we didn't provide its spatial distribution map of $r_p$.

In contrast to TXx and TNn, all influencing factors had significant impacts on TMm in the YRD. Due to the areas affected by GP were too small (about 3.25%, $r_p$ ranged from − 0.28 to − 0.37), and mainly distributed in Zhoushan, we didn't provide its spatial distribution map of $r_p$ with TMm, either. Based on the spatial distribution maps of the remaining six factors (Fig. 5g–l), TMm of the Jiangsu province was mainly influenced by atmospheric circulations, particularly APVA (Fig. 5g, about 42.83%, $r_p$ ranged from-0.28 to − 0.55) and EAZ (Fig. 5i, about 69.08%, $r_p$ ranged from 0.28 to 0.62). However, different regions were dominated by diverse atmospheric circulations. For example, the northern, middle and southern areas were dominated by EAZ and CA (Fig. 5k, about 17.35%, $r_p$ ranged from − 0.28 to − 0.31), WPHA (Fig. 5h, about 14.93%, $r_p$ ranged from 0.28 to 0.33) and EAM (Fig. 5j, about 23.57%, $r_p$ ranged from − 0.28 to − 0.42), and APVA, respectively. Similarly, GDP (Fig. 5l, about 91.93%, $r_p$ ranged from 0.28 to 0.57) had a great and wide impact on TMm in the YRD, especially for the southern coastal areas.

Overall, the partial correlation coefficients ($r_p$) between 3 temperature indices and 7 aforementioned factors, could partly explain the causes of the extreme temperature variations in the YRD. WPHA and CA had the respective strong correlations with TXx and TNn in the YRD. While GDP impacted all 3 temperature indices, mainly located in the southern YRD. This finding was in accordance with the findings illustrated in Jiang and Sun (2012) that temperature changes were positively correlated with WPHA and negatively correlated with APVA. Besides, the spatial distributions of partial correlation coefficients ($r_p$) between 3 temperature indices and 7 influencing factors revealed that changes of maximum temperature (TXx) were more caused by anthropogenic factors, while minimum temperature (TNn) was affected by natural environment. For mean temperature (TMm), it seemed to be comprehensively influenced by two groups of factors. This results could support the points of Zhang et al. (2011) that maximum temperature was more influenced by human activities, but minimum temperature was subject to influences of variations of net solar radiation for China. It was worth noting that the partial correlation coefficient ($r_p$) for 3 temperature indices and 7 influencing factors were not significant in the northern area of YRD. That might be attributed to the plain topography in these areas. According to Pepin et al. (2015), the climate response to greenhouse-gas forcing within complex mountain topography could be amplified in the mountain environment, rather than the flat terrain areas. In addition, GDP presented a greater and larger influence than GP in the YRD, which was contrary to the research of Balling et al. (2016) that natural logarithm of population increase impacted the maximum temperature, not the minimum temperature for Iran.

Thus it could be concluded that the influencing factors on long-term temperature change varied by region and the uncertainty was still great (Zhang et al., 2011). In addition, many researchers have also paid more attentions to the causes of the climate change and already made many notable achievements, though they mostly carried out the research from the single factor. With regard to natural factors, not only atmospheric circulations (Ruml et al., 2017) but also other factors, like net solar radiation (Zhang et al., 2011), volcanic explosion (Allen et al., 2015) and so on, might have considerable impacts on the climate change. And for anthropogenic factors, urbanization could be a greater comprehensive expression of all aspects, such as greenhouse gas emissions (IPCC, 2014), land use change (Yang et al., 2009), and so on.

## 5. Conclusions

In this study, we thoroughly analyzed the spatio-temporal variation and its influencing factors of temperature extremes across Yangtze River Delta China at the pixel scale during 1958–2014. The trends for the temperature series were detected with the Mann-Kendall trend test technique. The partial correlation coefficients between 3 temperature indices and 5 atmospheric circulation indexes, and 2 anthropogenic activity indicators were used to illustrate the different impacts from natural conditions and human factors on the local long-term temperature variation in the YRD. There existed obvious fluctuations and an overall increasing trend, particularly a sharp rise after 1990s, at the entire YRD regional scale for extreme maximum temperature (TXx, 0.41 °C/10 a), extreme minimum temperature (TNn, 0.52 °C/10 a) and mean temperature (TMm, 0.31 °C/10 a). The areas with significant increasing trends of TXx, TNn and TMm were 62.17%, 96.75% and 97.05% of the total YRD, respectively. There was a large spatial heterogeneity for TXx, TNn and TMm, with the characteristics of warmer in the midland and colder in the northern and the mountainous areas. It was mainly related to the geographical environment, such as geographical location, topography and land-sea distribution.

The partial correlation coefficients illustrated that TXx over YRD was mainly influenced by anthropogenic activities (economic development), while TNn was more affected by atmospheric circulations (e.g., the Eurasian zonal circulation index (EAZ) and the cold air activity index (CA)). For TMm, it was influenced by both atmospheric circulations and anthropogenic activities (− 0.33 for APVA, 0.28 for EAZ and 0.50 for GDP). As far as the spatial distributions of their affected areas, the northern YRD was mainly dominated by atmospheric circulations, while the southern YRD was more affected by anthropogenic activities.

Overall, the present study represented a close look at long-term

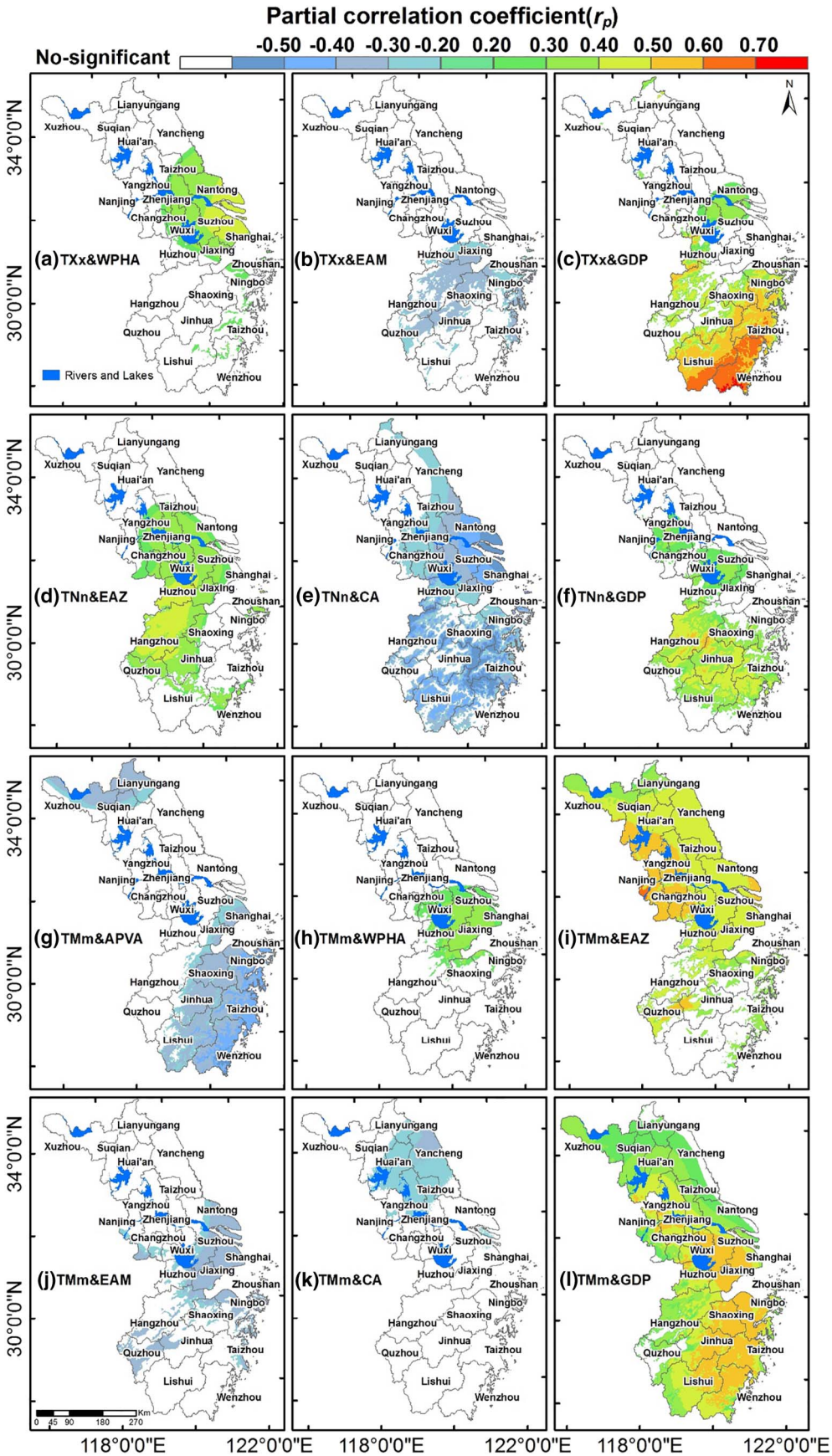


**Fig. 5.** The partial correlation coefficients ($r_p$) between 3 temperature indices and 7 influencing factors at the regional scale during 1958–2014. TXx: extreme maximum temperature, TNn: extreme minimum temperature, TMm: mean temperature, APVA: The Asia polar vortex area index, WPHA: The Western Pacific subtropical high area index, EAZ: The Eurasian zonal circulation index, EAM: The Eurasian meridional circulation index, CA: The cold air activity index, GDP: The gross domestic product. All partial correlation coefficients were significant at the 0.05 level and no-significant were the white areas. The rest maps were not illustrated as the correlations were not significant.

variations in temperature and their responses to climatic and human activities during 1958–2014 in the YRD. For the influencing factors, we mainly analyzed the atmospheric circulations and anthropogenic activities, such as the growth of the economic and population increasing. And we may not have taken other important factors into account due to data availability and integrity in the YRD, such as solar radiation, cloud coverage, and land use changes, and so on. Therefore, a strategy that combines and utilizes a network of multi-source data is required to fully address the problem.

## Acknowledgements

This study was supported by the National Natural Science Foundation of China (41471076) and Key Laboratory of Spatial Data Mining & Information Sharing of Ministry of Education, Fuzhou University (No. 2017LSDMIS07). The authors would thank the National Climate Center of the China Meteorological Administration and the National Climatic Data Center of the National Oceanic and Atmospheric Administration for providing the meteorological data, the Institute of Geographic Sciences and Natural Resources Research for providing the DEM data, the Climate Diagnostics and Prediction Division of the National Climate Center for providing the atmospheric circulation data, and the National Bureau of Statistics of China for providing the statistical data for this study.

## Appendix 1. Metrological stations in the YRD

| Station code | Station name | Province | Latitude (°N) | Longitude (°E) | Elevation (m) |
|---|---|---|---|---|---|
| 58,026 | Pizhou | Jiangsu | 34.40 | 118.02 | 25.95 |
| 58,027 | Xuzhou | Jiangsu | 34.28 | 117.15 | 52.88 |
| 58,038 | Muyang | Jiangsu | 34.08 | 118.78 | 5.75 |
| 58,040 | Ganyu | Jiangsu | 34.85 | 119.13 | 4.90 |
| 58,047 | Guanyun | Jiangsu | 34.25 | 119.23 | 3.59 |
| 58,130 | Suining | Jiangsu | 33.93 | 117.95 | 22.25 |
| 58,135 | Sihong | Jiangsu | 33.48 | 118.22 | 16.57 |
| 58,138 | Xuyi | Jiangsu | 32.98 | 118.52 | 27.14 |
| 58,141 | Huaian | Jiangsu | 33.63 | 118.93 | 11.19 |
| 58,143 | Funing | Jiangsu | 33.80 | 119.85 | 1.67 |
| 58,144 | Qingjiang | Jiangsu | 33.59 | 119.02 | 12.22 |
| 58,150 | Sheyang | Jiangsu | 33.75 | 120.30 | 2.69 |
| 58,158 | Dafeng | Jiangsu | 33.20 | 120.48 | 3.24 |
| 58,238 | Nanjing | Jiangsu | 31.93 | 118.90 | 23.39 |
| 58,241 | Gaoyou | Jiangsu | 32.80 | 119.45 | 4.43 |
| 58,251 | Dongtai | Jiangsu | 32.85 | 120.28 | 2.95 |
| 58,255 | Rugao | Jiangsu | 32.37 | 120.57 | 5.49 |
| 58,259 | Nantong | Jiangsu | 32.08 | 120.98 | 7.75 |
| 58,265 | Lvsi | Jiangsu | 32.07 | 121.60 | 1.07 |
| 58,343 | Changzhou | Jiangsu | 31.88 | 119.98 | 5.03 |
| 58,345 | Liyang | Jiangsu | 31.43 | 119.50 | 4.88 |
| 58,354 | Wuxi | Jiangsu | 31.62 | 120.35 | 3.22 |
| 58,356 | Kunshan | Jiangsu | 31.40 | 121.00 | 2.06 |
| 58,358 | Dongshan | Jiangsu | 31.07 | 120.43 | 4.19 |
| 58,362 | Baoshan | Shanghai | 31.40 | 121.45 | − 0.39 |
| 58,367 | Xujiahui | Shanghai | 31.19 | 121.42 | 1.10 |
| 58,445 | Tianmushan | Zhejiang | 30.34 | 119.41 | 1145.87 |
| 58,448 | Lin'an | Zhejiang | 30.22 | 119.70 | 55.44 |
| 58,450 | Huzhou | Zhejiang | 30.87 | 120.05 | 50.00 |
| 58,457 | Hangzhou | Zhejiang | 30.23 | 120.17 | 50.83 |
| 58,464 | Pinhu | Zhejiang | 30.65 | 121.12 | 31.43 |
| 58,467 | Cixi | Zhejiang | 30.20 | 121.27 | 26.25 |
| 58,472 | Shengsi | Zhejiang | 30.73 | 122.44 | 47.16 |
| 58,473 | Shengshan | Zhejiang | 30.72 | 122.81 | 25.10 |
| 58,477 | Dinghai | Zhejiang | 30.03 | 122.10 | 91.84 |
| 58,543 | Chun'an | Zhejiang | 29.62 | 119.02 | 140.01 |
| 58,549 | Jinhua | Zhejiang | 29.12 | 119.65 | 50.35 |
| 58,553 | Shangyu | Zhejiang | 30.05 | 120.82 | 50.00 |
| 58,556 | Shengzhou | Zhejiang | 29.60 | 120.82 | 63.39 |
| 58,557 | Yiwu | Zhejiang | 29.33 | 120.08 | 100.00 |
| 58,562 | Yinzhou | Zhejiang | 29.78 | 121.55 | 26.09 |
| 58,569 | Shipu | Zhejiang | 29.20 | 121.96 | 25.87 |
| 58,633 | Quzhou | Zhejiang | 29.00 | 118.90 | 98.47 |
| 58,646 | Lishui | Zhejiang | 28.47 | 119.93 | 83.30 |
| 58,647 | Longquan | Zhejiang | 28.06 | 119.12 | 222.29 |
| 58,652 | Xianju | Zhejiang | 28.87 | 120.72 | 109.28 |
| 58,653 | Kuocangshan | Zhejiang | 28.81 | 120.91 | 811.37 |

| | | | | | |
|---|---|---|---|---|---|
| 58,659 | Wenzhou | Zhejiang | 28.02 | 120.64 | 50.00 |
| 58,660 | Linhai | Zhejiang | 28.84 | 121.12 | 56.33 |
| 58,665 | Hongjia | Zhejiang | 28.62 | 121.42 | 49.29 |
| 58,666 | Dachen | Zhejiang | 28.45 | 121.90 | 30.39 |
| 58,667 | Yuhuan | Zhejiang | 28.08 | 121.27 | 52.75 |
| 58,742 | Yunhe | Zhejiang | 28.10 | 119.57 | 156.79 |
| 58,752 | Rui'an | Zhejiang | 27.78 | 120.65 | 54.01 |
| 58,760 | Dongtou | Zhejiang | 27.83 | 121.15 | 54.73 |
| 58,765 | Beilu | Zhejiang | 27.63 | 121.21 | 6.63 |

## References


Alexander, L.V., Zhang, X., Peterson, T.C., Caesar, J., Gleason, B., Klein Tank, A.M.G., Haylock, M., Collins, D., Trewin, B., Rahimzadeh, F., 2006. Global observed changes in daily climate extremes of temperature and precipitation. J. Geophys. Res. Atmos. 111, 1042–1063.

Allen, S.M.J., Gough, W.A., Mohsin, T., 2015. Changes in the frequency of extreme temperature records for Toronto, Ontario, Canada. Theor. Appl. Climatol. 119, 481–491.

Arnell, N.W., 1999. Climate change and global water resources. Glob. Environ. Change. 9, S31–S49.

Ballester, J., Giorgi, F., Rodo, X., 2010. Changes in European temperature extremes can be predicted from changes in PDF central statistics. Clim. Chang. 98, 277–284.

Balling Jr., R.C., Kiany, M.S.K., Roy, S.S., 2016. Anthropogenic signals in Iranian extreme temperature indices. Atmos. Res. 169, 96–101.

Bonsal, B.R., Zhang, X., Vincent, L.A., Hogg, W.D., 2001. Characteristics of daily and extreme temperatures over Canada. J. Clim. 14, 1959–1976.

Chen, H.B., Fan, X.H., 2007. Some extreme events of weather, climate and related phenomena in 2006. Clim. Environ. Res. (in Chinese) 13, 102–112.

Donat, M.G., Alexander, L.V., Yang, H., Durre, I., Vose, R., Dunn, R.J.H., Willett, K.M., Aguilar, E., Brunet, M., Caesar, J., Hewitson, B., Jack, C., Klein Tank, A.M.G., Kruger, A.C., Marengo, J., Peterson, T.C., Renom, M., Oria Rojas, C., Rusticucci, M., Salinger, J., Elrayah, A.S., Sekele, S.S., Srivastava, A.K., Trewin, B., Villarroel, C., Vincent, L.A., Zhai, P., Zhang, X., Kitching, S., 2013. Updated analyses of temperature and precipitation extreme indices since the beginning of the twentieth century: the HadEX2 dataset. J. Geophys. Res. Atmos. 118, 2098–2118.

Du, Y., Xie, Z., Zeng, Y., Shi, Y., Wu, J., 2007. Impact of urban expansion on regional temperature change in the Yangtze River Delta. J. Geogr. Sci. 17, 387–398.

Gao, J., Sun, Y., Liu, Q., Zhou, M., Lu, Y., Li, L., 2015. Impact of extreme high temperature on mortality and regional level definition of heat wave: a multi-city study in China. Sci. Total Environ. 505, 535–544.

Gocic, M., Trajkovic, S., 2013. Analysis of changes in meteorological variables using Mann-Kendall and Sen's slope estimator statistical tests in Serbia. Glob. Planet. Chang. 100, 172–182.

Gönençgil, B., Deniz, Z.A., 2016. Extreme maximum and minimum air temperature in Mediterranean coasts in Turkey. Geogr. Environ. Sustain. (in Chinese) 9, 59–70.

Hutchinson, M.F., 1999. ANUSPLIN Version 4.0. http://cres.anu.edu.au/software/anusplin.html.

IPCC, 2013. Climate Change 2013: The Physical Science Basis. Contribution of Working Group I to the Fifth Assessment Report of the Intergovernmental Panel on Climate Change. Cambridge University Press, Cambridge, United Kingdom, pp. 3–29.

IPCC, 2014. Climate Change 2014: Synthesis Report. Contribution of Working Groups I, II and III to the Fifth Assessment Report of the Intergovernmental Panel on Climate Change. Cambridge University Press, Cambridge, United Kingdom, pp. 2–164.

Iqbal, M.A., Penas, A., Canoortiz, A., Kersebaum, K.C., Herrero, L., Del Río, S., 2016. Analysis of recent changes in maximum and minimum temperatures in Pakistan. Atmos. Res. 168, 234–249.

Jansen, J.M., Pronker, A.E., Kube, S., Sokolowski, A., Sola, J.C., Marquiegui, M.A., Schiedek, D., Wendelaar Bonga, S., Wolowicz, M., Hummel, H., 2007. Geographic and seasonal patterns and limits on the adaptive response to temperature of European *Mytilus* spp. and *Macoma balthica* populations. Oecologia 154, 23–34.

Jiang, J.J., Sun, W., 2012. Climate change and possible reasons in Yangtze River Region in recent 50 years. Meteorol. Disas. Reduc. Res. (in Chinese) 35, 17–25.

Jones, G.V., 2005. Climate change in the Western United States grape growing regions. Acta Hortic. 689.

Kadioğlu, M., Şen, Z., Gültekin, L., 2001. Variations and trends in Turkish seasonal heating and cooling degree-days. Clim. Chang. 49, 209–223.

Karl, T.R., Nicholls, N., Ghazi, A., 1999. Clivar/GCOS/WMO workshop on indices and indicators for climate extremes workshop summary. Clim. Chang. 42, 3–7.

Kendall, M.G., 1962. Rank Correlation Methods. Hafner Publishing Company, New York.

Kilibarda, M., Hengl, T., Heuvelink, G.B.M., Gräler, B., Pebesma, E., Perčec Tadić, M., Bajat, B., 2014. Spatio-temporal interpolation of daily temperatures for global land areas at 1 km resolution. J. Geophys. Res. 119, 2294–2313.

Mann, H.B., 1945. Nonparametric tests against trend. Econometrica 13, 245–259.

Moberg, A., Jones, P.D., Lister, D., Walther, A., Brunet, M., Jacobeit, J., Alexander, L.V., Della-Marta, P.M., Luterbacher, J., Yiou, P., 2006. Indices for daily temperature and precipitation extremes in Europe analyzed for the period 1901–2000. J. Geophys. Res. Atmos. 111, 5295–5305.

National Bureau of Statistics of China, 1959–2015. China Statistical Yearbook 1959–2015. China Statistical Press, Beijing, China.

National Bureau of Statistics of China, 2015. China Statistical Yearbook 2015,2015. China Statistical Press, Beijing, China.

Ogden, N.H., Radojevic, M., Wu, X., Duvvuri, V.R., Leighton, P.A., Wu, J., 2014. Estimated effects of projected climate change on the basic reproductive number of the Lyme disease vector *Ixodes scapularis*. Environ. Health Perspect. 122, 631–638.

Papakostas, K., Bentoulis, A., Bakas, V., Kyriakis, N., 2007. Estimation of ambient temperature bin data from monthly average temperatures and solar clearness index. Validation of the methodology in two Greek cities. Renew. Energ. 32, 991–1005.

Peng, J.B., 2014. An investigation of the formation of the heat wave in Southeast China in summer 2013 and the relevant abnormal subtropical high activities. Atmos. Ocean. Sci. Lett. (in Chinese) 7, 286–290.

Pepin, N., Bradley, R.S., Diaz, H.F., Baraer, M., Caceres, E.B., Forsythe, N., Fowler, H., Greenwood, G., Hashmi, M.Z., Liu, X.D., Miller, J.R., Ning, L., Ohmura, A., Palazzi, E., Rangwala, I., Schöner, W., Severskiy, I., Shahgedanova, M., Wang, M.B., Williamson, S.N., Yang, D.Q., 2015. Elevation-dependent warming in mountain regions of the world. Nat. Clim. Chang. 5, 424–430.

Robine, J.M., Cheung, S.L., Le Roy, S., Van Oyen, H., Griffiths, C., Michel, J.P., Herrmann, F.R., 2008. Death toll exceeded 70,000 in Europe during the summer of 2003. C. R. Biol. 331, 171–178.

Ruml, M., Gregorić, E., Vujadinović, M., Radovanović, S., Matović, G., Vuković, A., Počuča, V., Stojičić, D., 2017. Observed changes of temperature extremes in Serbia over the period 1961 − 2010. Atmos. Res. 183, 26–41.

Sang, Y.F., 2012. Spatial and temporal variability of daily temperature in the Yangtze River Delta, China. Atmos. Res. 112, 12–24.

Sen, P.K., 1968. Estimates of the regression coefficient based on Kendall's tau. J. Am. Stat. Assoc. 63, 1379–1389.

Seneviratne, S.I., Nicholls, N., Easterling, D., Goodess, C.M., Kanae, S., Kossin, J., Luo, Y., Marengo, J., Mcinnes, K., Rahimi, M., 2012. Changes in climate extremes and their impacts on the natural physical environment: an overview of the IPCC SREX report. EGU General Assembly Conference 12566.

Shi, J., Ding, Y.H., Cui, L.L., 2009. Climatic characteristics of extreme maximum temperature in East China and its causes. Chin. J. Atmos. Sci. (in Chinese) 33, 347–358.

Stone, B., Hess, J.J., Frumkin, H., 2010. Urban form and extreme heat events: are sprawling cities more vulnerable to climate change than compact cities? Environ. Health Perspect. 118, 1425–1428.

Sun, Q.L., Feng, X.F., Yong, G., Li, B.L., 2015. Topographical effects of climate data and their impacts on the estimation of net primary productivity in complex terrain: a case study in Wuling mountainous area, China. Ecol. Inform. 27, 44–54.

Sun, W.Y., Mu, X.M., Song, X.Y., Wu, D., Cheng, A.F., Qiu, B., 2016. Changes in extreme temeperature and precipitation events in the Loess Plateau (China) during 1960–2013 under global warming. Atmos. Res. 168, 33–48.

Wang, Q., Zhang, M., Wang, S., Ma, Q., Sun, M., 2014. Changes in temperature extremes in the Yangtze River Basin, 1962–2011. J. Geogr. Sci. 24, 59–75.

Xie, Z.Q., Du, Y., Zeng, Y., Yan, M.L., Zhu, C.Y., 2010. Accelerated human activities affecting the spatial pattern of temperature in the Yangtze River Delta. Quatern. Int. 226, 112–121.

Yang, X.C., Zhang, Y.L., Liu, L.S., Zhang, W., Ding, M.J., Wang, Z.F., 2009. Sensitivity of surface air temperature change to land use/cover types in China. Sci. China Ser. D-Earth. Sci. (in Chinese) 52, 1207–1215.

Yu, K., Xie, S.P., 2013. Recent global-warming hiatus tied to equatorial Pacific surface cooling. Nature 501, 403–407.

Yu, P.S., Yang, T.C., Chou, C.C., 2002. Effects of climate change on evapotranspiration from paddy fields in southern Taiwan. Clim. Chang. 54, 165–179.

Zhang, N., Gao, Z., Wang, X., Chen, Y., 2010. Modeling the impact of urbanization on the local and regional climate in Yangtze River Delta, China. Theor. Appl. Climatol. 102, 331–342.

Zhang, Q., Li, J., Chen, Y.D., Chen, X., 2011. Observed changes of temperature extremes during 1960–2005 in China: natural or human-induced variations? Theor. Appl. Climatol. 106, 417–431.

Zhou, S., Miller, A.J., Hood, L.L., 2000. A partial correlation analysis of the stratospheric ozone response to 27-day solar UV variations with temperature effect removed. J. Geophys. Res. Atmos. (in Chinese) 105, 4491–4500.

Zhu, X., He, H., Min, L., Yu, G., Sun, X., 2010. Spatio-temporal variation of photosynthetically active radiation in China in recent 50 years. J. Geogr. Sci. 20, 803–817.